(2)

JHU/APL
TG 1383
AUGUST 1992

Technical Memorandum

A NEW MODEL FOR INTERPRETING EXPERIMENTAL DATA FROM A CIRCULAR WAVEGUIDE CAVITY

WILLIAM A. HUTING

THE JOHNS HOPKINS UNIVERSITY ■ APPLIED PHYSICS LABORATORY

JHU/APL
TG 1383
AUGUST 1992

Technical Memorandum

A NEW MODEL FOR INTERPRETING EXPERIMENTAL DATA FROM A CIRCULAR WAVEGUIDE CAVITY

WILLIAM A. HUTING

THE JOHNS HOPKINS UNIVERSITY ■ APPLIED PHYSICS LABORATORY
Johns Hopkins Road, Laurel, Maryland 20723-6099
Operating under Contract N00039-91-C-0001 with the Department of the Navy

UNCLASSIFIED

SECURITY CLASSIFICATION OF THIS PAGE

REPORT DOCUMENTATION PAGE

1a. REPORT SECURITY CLASSIFICATION
UNCLASSIFIED

1b. RESTRICTIVE MARKINGS

2a. SECURITY CLASSIFICATION AUTHORITY

2b. DECLASSIFICATION/DOWNGRADING SCHEDULE

3. DISTRIBUTION/AVAILABILITY OF REPORT
Approved for public release; distribution unlimited

4. PERFORMING ORGANIZATION REPORT NUMBER(S)
JHU/APL TG-1383

5. MONITORING ORGANIZATION REPORT NUMBER(S)
JHU/APL TG-1383

6a. NAME OF PERFORMING ORGANIZATION
The Johns Hopkins University
Applied Physics Laboratory

6b. OFFICE SYMBOL (If applicable)
TIR

7a. NAME OF MONITORING ORGANIZATION
The Johns Hopkins University
Applied Physics Laboratory

6c. ADDRESS (City, State, and ZIP Code)
Johns Hopkins Road
Laurel, Md. 20723-6099

7b. ADDRESS (City, State, and ZIP Code)
Johns Hopkins Road
Laurel, Md. 20723-6099

8a. NAME OF FUNDING/SPONSORING ORGANIZATION
Dept. of the Navy
Naval Sea Systems Command O6C

8b. OFFICE SYMBOL (If applicable)

9. PROCUREMENT INSTRUMENT IDENTIFICATION NUMBER
N00039-91-C-0001

8c. ADDRESS (City, State, and ZIP Code)
NC-2 Crystal City, Va. 20362

10. SOURCE OF FUNDING NUMBERS

PROGRAM ELEMENT NO.	PROJECT NO.	TASK NO.	WORK UNIT ACCESSION NO.
		BKHR9LXX F2F	

11. TITLE (Include Security Classification)
A New Model for Interpreting Experimental Data from a Circular Waveguide Cavity (U)

12. PERSONAL AUTHOR(S)
William A. Huting

13a. TYPE OF REPORT	13b. TIME COVERED	14. DATE OF REPORT (Year, Month, Day)	15. PAGE COUNT
Technical Memorandum	FROM ________ TO ________	92-8-7	20

16. SUPPLEMENTARY NOTATION

17. COSATI CODES

FIELD	GROUP	SUB-GROUP

18. SUBJECT TERMS (Continue on reverse if necessary and identify by block number)
Waveguide
Resonator
Attenuation
Microwaves

19. ABSTRACT (Continue on reverse if necessary and identify by block number)

Progress is described in the testing of circular TE_{01} waveguide using a resonant cavity technique. A new model has been developed for extrapolating insertion loss values from experimental cavity Q data. This model is compared with a previous model, and experiments are described that involve both cavities with mechanically adjustable lengths and cavities with fixed lengths. Data are also presented for waveguide bend cavities. In all cases, the extrapolated traveling wave losses were in good agreement with the theory.

20. DISTRIBUTION/AVAILABILITY OF ABSTRACT
☒ UNCLASSIFIED/UNLIMITED ☐ SAME AS RPT. ☐ DTIC USERS

21. ABSTRACT SECURITY CLASSIFICATION
UNCLASSIFIED

22a. NAME OF RESPONSIBLE INDIVIDUAL
NAVTECH REP Security Officer

22b. TELEPHONE (Include Area Code)
(301) 953-5403

22c. OFFICE SYMBOL
NAVTECH REP

DD FORM 1473, 84 MAR

83 APR edition may be used until exhausted
All other editions are obsolete.

SECURITY CLASSIFICATION OF THIS PAGE
UNCLASSIFIED

ABSTRACT

Progress is described in the testing of circular TE_{01} waveguide using a resonant cavity technique. A new model has been developed for extrapolating insertion loss values from experimental cavity Q data. This model is compared with a previous model, and experiments are described that involve both cavities with mechanically adjustable lengths and cavities with fixed lengths. Data are also presented for waveguide bend cavities. In all cases, the extrapolated traveling wave losses were in good agreement with the theory.

CONTENTS

ILLUSTRATIONS

TABLES

1. INTRODUCTION

Circular TE_{01} waveguide is currently being investigated for low-loss use, and this paper describes progress in the testing of such waveguide using a resonant cavity technique. This technique is useful because long lengths of waveguide are not always available for testing, and the attenuation in short sections of waveguide can be too small to measure directly. An alternative is to convert a short waveguide section into a variable-length cavity by attaching a metal plate to one end and inserting a conducting piston into the other end as shown in Figure 1. Q data (the Q, or Quality Factor, of a cavity is the resonant frequency divided by the 3-dB bandwidth of the cavity excitation response) are then obtained at several resonant lengths for a fixed center frequency.[1] The next step is to compute a numerical value for the traveling wave insertion loss from these Q data.

In this paper, a new relation is derived for extrapolating an insertion loss figure from the cavity Q figures, and this new model is compared with an older one published by Karbowiak and Skedd.[1] Test results are also presented. The new model can also be modified for use in determining the insertion loss of nonuniform waveguide sections. For example, a 90° circular–cross-section waveguide bend has been tested at 3.3 GHz. Q data indicate a loss that is in good agreement with previous theory. Finally, the potential applicability of the new model to the problem of using fixed-length cavities to determine waveguide attenuation is described.

The waveguide sections tested were made of sheathed-helix waveguide (see Fig. 2). This waveguide consists of a tightly wound insulated wire surrounded by a lossy dielectric, which is in turn encapsulated by a good conductor. The purpose of this

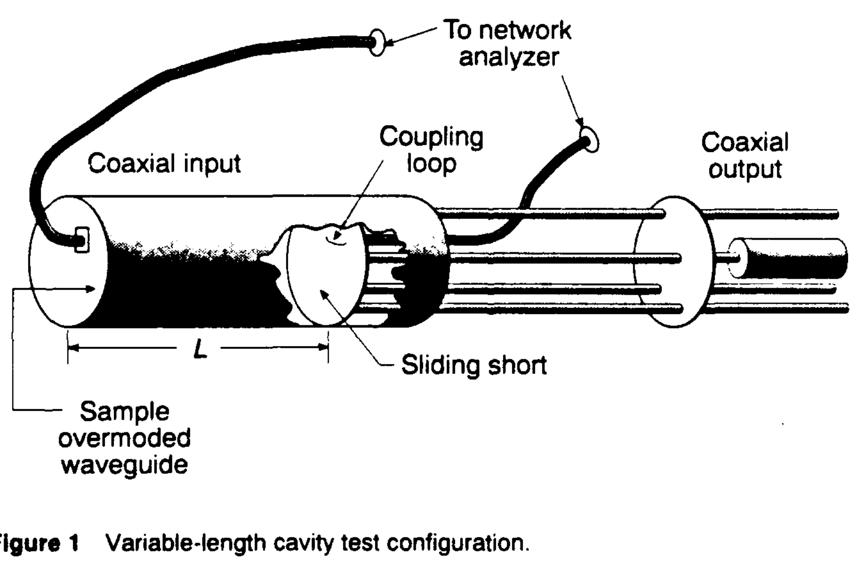

Figure 1 Variable-length cavity test configuration.

[1]A. E. Karbowiak, and R. F. Skedd, "Testing of Circular Waveguides Using a Resonant Cavity Method," *Proc. IEE* **106B**, Supplement 13, 66–70 (Sep 1959).

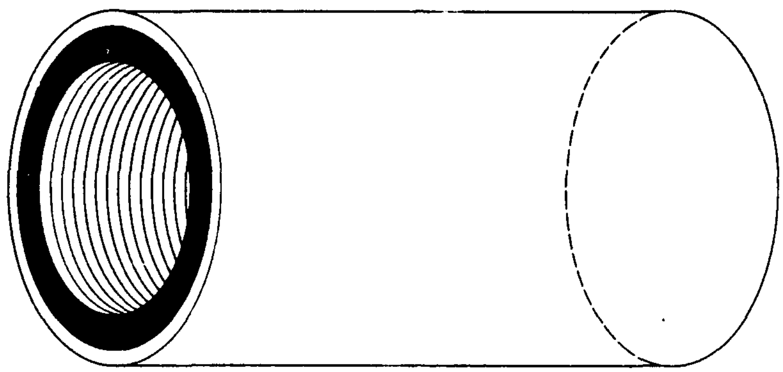

Figure 2 Sheathed-helix waveguide.

configuration is to suppress all the modes except the TE_{01} mode. Various design and development issues are described in Reference 2. Methods for establishing theoretical insertion losses for these devices are also given in Reference 2.

2. VARIABLE–LENGTH STRAIGHT CAVITIES

In this paper, tests are described that quantify insertion loss for circular overmoded waveguide. The two basic test configurations are shown in Figures 1 and 3. Figure 3 depicts a traveling wave test configuration, which is made possible by using a rectangular TE_{10} to circular TE_{01} mode transducing waveguide section. The transition used in these tests was the Marie transducer,[3] a device discussed at some length in References 4 and 5. Unfortunately, precise determination of insertion losses for relatively short sections of waveguide using this setup is not practical because the predicted low losses are beyond the sensitivity of the measurement apparatus. This configuration is very useful, however, in investigating bends, as will be discussed later in this paper. All the experimental data presented herein were obtained using an automatic network analyzer.

Tests using the configuration presented in Figure 1 will now be described. Initially, the endplates were of the type depicted in Figure 4 with a coupling half-loop located

[2]W. A. Huting, J. W. Warren, and J. A. Krill, "Recent Progress in Circular High-Power Overmoded Waveguide," *Johns Hopkins APL Tech. Dig.* **12**(1), 60–74 (1991).
[3]G. R. P. Marie, *Mode Transforming Waveguide Transition*, U. S. Patent No. 2,859,412, 4 Nov 1958.
[4]S. S. Saad, J. B. Davies, and O. J. Davies, "Analysis and Design of a Circular TE_{01} Mode Transducer," *IEE J. Microwaves Opt. Acoust.* **1**, 58–62 (Jan 1977).
[5]S. S. Saad, J. B. Davies, and O. J. Davies, "Computer Analysis of Gradually Tapered Waveguide with Arbitrary Cross Sections," *IEEE Trans. on Microwaves Theory Tech.* **MTT-25**, 437–440 (May 1977).

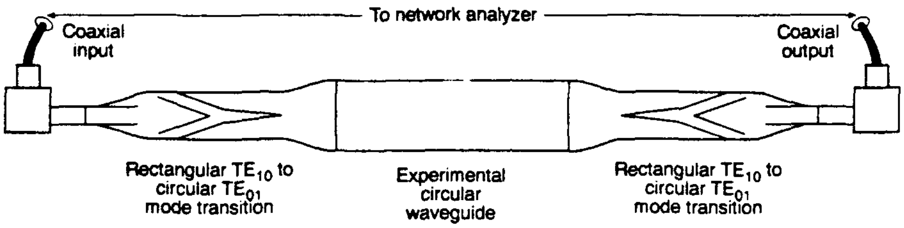

Figure 3 Traveling wave test configuration.

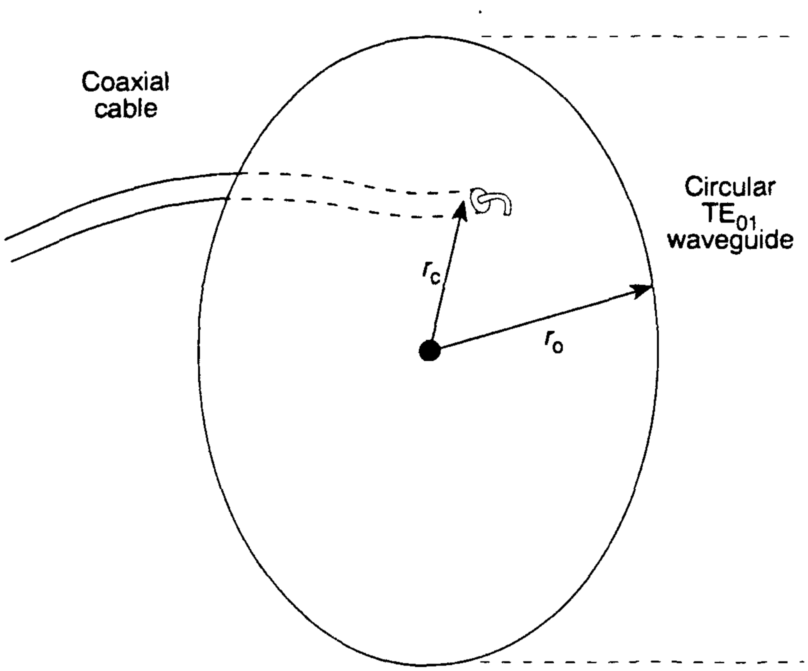

Figure 4 Endplate used in variable-length cavity tests. The plane of the coupling loop was perpendicular to the radius vector, and $r_c = 0.4804\ r_o$.

slightly off-center between the cavity axis and the helix to maximize TE_{01} coupling. As a first step in constructing a theoretical model for this cavity, one may define a 2×2 scattering matrix describing the cavity endplates, which are assumed to be identical. The subscript "1" refers to the TEM mode of the coaxial line, and the subscript "2" refers to the TE_{01} mode of the circular waveguide as shown in Figure 5. The scattering parameters of this system are denoted S_{11}, S_{12}, S_{21}, and S_{22}. A simple cascading formulation (see Ref. 6) may be used to determine the transmission coefficient T of the entire system (i.e., Fig. 6):

[6]R. H. Dicke, "General Microwave Theorems," in *Principles of Microwave Circuits*, C. G. Montgomery, R. H. Dicke, and E. M. Purcell (eds.), McGraw-Hill, New York, pp. 130–161 (1948).

$$T = \frac{S_{12}^2}{-S_{22}^2 \exp(-\alpha_{01}L)\exp(-j\beta_{01}L) + \exp(\alpha_{01}L)\exp(j\beta_{01}L)}, \quad (1)$$

where α_{01} is the TE_{01} attenuation, β_{01} is the TE_{01} wave number, and L is the cavity length. Let ω_o be the resonant frequency of a perfectly conducting cavity. Computing the magnitude of T and expanding $\exp(\pm j\beta_{01}L)$ in a Taylor series about $\omega = \omega_o$, one obtains an expression in this form:

$$|T|^2 = \frac{K}{(\omega - \omega_o - \delta\omega)^2 + \left(\frac{\omega_o + \delta\omega}{2Q}\right)^2}. \quad (2)$$

Here, the transmission coefficient T has a 3-dB bandwidth equal to $(\omega_o + \delta\omega)/Q$, K is a parameter independent of frequency, and $\delta\omega$ is the (extremely small) shift of the resonant frequency due to losses. Expressions in the form of Equation 2 are discussed in many textbooks (e.g., Ref. 7, p. 357). The previously mentioned expansion of $\exp(\pm j\beta_{01}L)$ also yields the following relations:

$$\delta\omega = \frac{S_{22r}S_{22i}\omega_o\beta_{01}^2(\omega_o)}{\left\{\left(S_{22r}^2 - S_{22i}^2\right)\omega_o^2\mu_o\epsilon_o L[\beta_{01}(\omega_o)] - S_{22r}S_{22i}\left[(\beta_{01}(\omega_o))^2 - \omega_o^2\mu_o\epsilon_o\right]\right\}} \quad (3)$$

and

$$\left(\frac{\omega_o + \delta\omega}{2Q}\right)^2 + (\delta\omega)^2 = \quad (4)$$

$$\frac{\left(S_{22r}^2 + S_{22i}^2\right)^2 \exp(-2\alpha_{01}L) + \exp(2\alpha_{01}L) - 2\left(S_{22r}^2 - S_{22i}^2\right)}{\left\{4\left(S_{22r}^2 - S_{22i}^2\right)L^2\omega_o^2\mu_o^2\epsilon_o^2 / [\beta_{01}(\omega_o)]^2 - 4 \times S_{22r}S_{22i}L\left[\frac{\mu_o\epsilon_o}{\beta_{01}(\omega_o)} - \frac{\omega_o^2\mu_o^2\epsilon_o^2}{[\beta_{01}(\omega_o)]^3}\right]\right\}}.$$

In Equations 3 and 4, the variables S_{mnr} and S_{mni} denote, respectively, the real and imaginary parts of the endplate scattering parameters, ϵ_o is the free-space permittivity, and μ_o is the free-space permeability. Equations 3 and 4 provide the relations for extracting values for α_{01} from the experimental data. For example, when a 2-ft-long, 16-cm-inner-diameter section of S-band helical waveguide was investigated, Q's were obtained at $(\omega_o + \delta\omega)/2\pi = 3.3$ GHz for nine resonant lengths. These data, when substituted into Equations 3 and 4, resulted in nine equations (corresponding to the nine measurements) in three unknowns: S_{22r}, S_{22i}, and α_{01}. Values for these parameters were established using a least-mean-squares approach, and, for five different cavities, the computed values for α_{01} were between 3% below and 74% above the theoretical value (0.00299 dB/m). As an alternative to this computationally intensive procedure,

[7] J. D. Jackson, *Classical Electrodynamics*, 2nd Ed., Wiley, New York (1975).

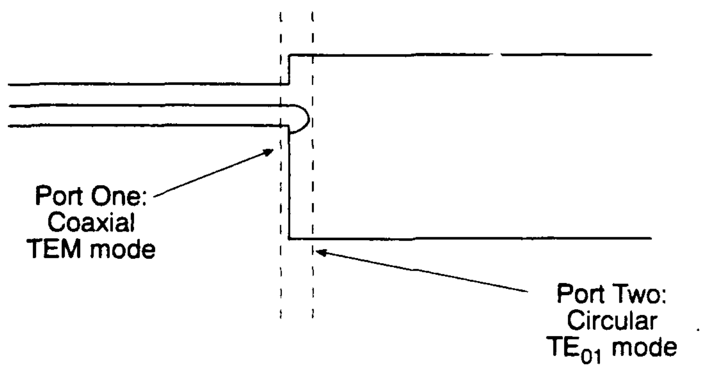

Figure 5 Reference ports for the scattering matrix $\begin{pmatrix} S_{11} & S_{12} \\ S_{21} & S_{22} \end{pmatrix}$.

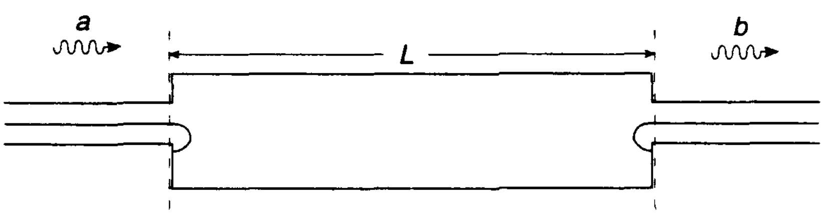

Figure 6 Generalized cavity geometry. Let *a* and *b* denote the forward-traveling TEM wave amplitudes at the input and output ends of the cavity. The transmission coefficient *T* is defined by $b = Ta$.

one might want to use the following simple linear relation originally given by Karbowiak and Skedd in Reference 1:

$$\Delta f = \frac{\lambda_o^2}{\pi \lambda_g} f_o \left(\alpha_{01} + \frac{C}{L} \right), \tag{5}$$

where

Δf = 3-dB bandwidth,
λ_o = free-space wavelength,
λ_g = guide wavelength,
f_o = resonant frequency,
C = a parameter independent of cavity length that is determined by the endplate properties, and
L = cavity length.

When a linear fit was applied to the nine points (Δf, $1/L$), the extrapolated values of α_{01} for the five different cavities were between 37% above and 75% above the theoretical attenuation. Figure 7 shows both experimental and numerical (Δf, $1/L$) data for one of the cavities. The numerical data were generated using these least-mean-square values: $\alpha_{01} = 0.00290$ dB/m, $S_{22r} = -0.9988$, and $S_{22i} = 0.0136$. The linear characteristic predicted by Karbowiak and Skedd is also predicted by the new model;

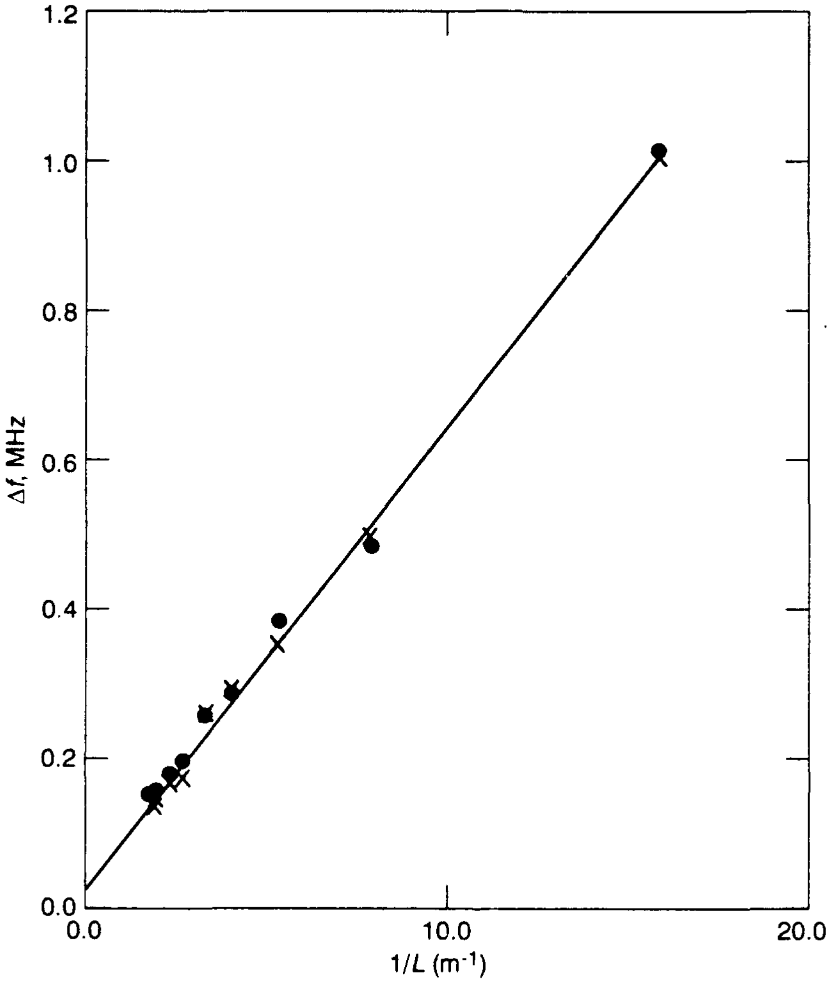

Figure 7 Experimental (x) and numerical (·) data for a 2-ft-long, 16-cm-inner-diameter sheathed-helix waveguide cavity at 3.3 GHz. The solid line is a linear fit of the experimental data. For this short cavity, Karbowiak's model and the new model are in good agreement.

moreover, the extrapolated α_{01} values are nearly the same in either model. Additionally, an 8-ft-long straight waveguide section has been investigated at 3.3 GHz. Performing a linear fit on the experimental data results in a line with a negative slope as shown in Figure 8; the extrapolated attenuation value is about ten times the theoretical value. Use of the new model, however, results in an attenuation of 0.00389 dB/m. Thus, the new model appears to be useful for both long and short cavities; the model of Karbowiak and Skedd appears to be useful only for short cavities.

Sources of possible measurement error will now be described. According to the network analyzer operating manual, transmission ($|T|^2$) measurements were accurate to within ±0.1 dB.[8] Substitution of these bounds into Equation 2 results in additional

[8]*Model 360 Vector Network Analyzer Operation Manual*, Revision C, Wiltron Company, Morgan Hill, Ca., p. 1-9 (1987).

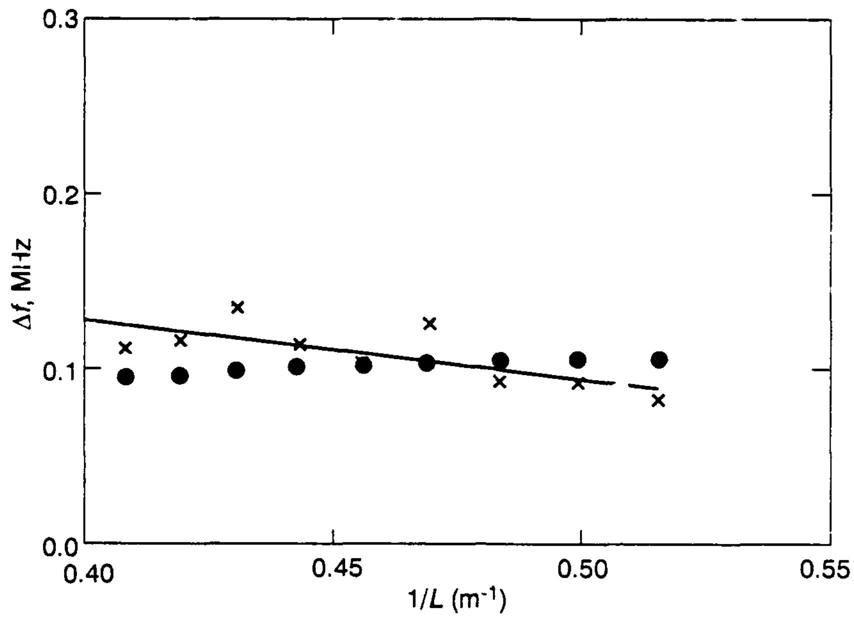

Figure 8 Experimental (x) and numerical (·) data for an 8-ft-long, 16-cm-inner-diameter sheathed-helix waveguide cavity at 3.3 GHz. The solid line is a linear fit of the experimental data. For this long cavity, the new model is in good agreement with theory but in poor agreement with Karbowiak's model.

bounds on the accuracy of the measured Q's and 3-dB bandwidths. One then allows the 3-dB bandwidth in Equation 5 to vary within these computed bounds in order to predict a range for the extrapolated insertion losses. When this was done for the S-band waveguide, the ratio between the highest and lowest extrapolated attenuations was approximately 1.5. This range is consistent with our data.

3. BEND CAVITIES

The methods described above may be modified to determine the transmission properties of a waveguide bend. One such bend, made out of circular sheathed-helix waveguide, is shown in Figure 9. The TE_{01} transmission coefficient of the bend will be denoted $\exp(-M/8.68)\exp(-j\Delta)$; M is the insertion loss in dB. The investigations of the bend were slightly complicated by the inability to push the straight piston in very far. Several ways of circumventing this difficulty exist. For example, one could begin by measuring the phase shift Δ of the bend to facilitate the far more important task of determining insertion loss. The phase shift and its derivative $d\Delta/d\omega$ may be obtained using the traveling wave setup of Figure 3. (The two Marie transducers must be measured directly connected to one another, and their combined phase shift is

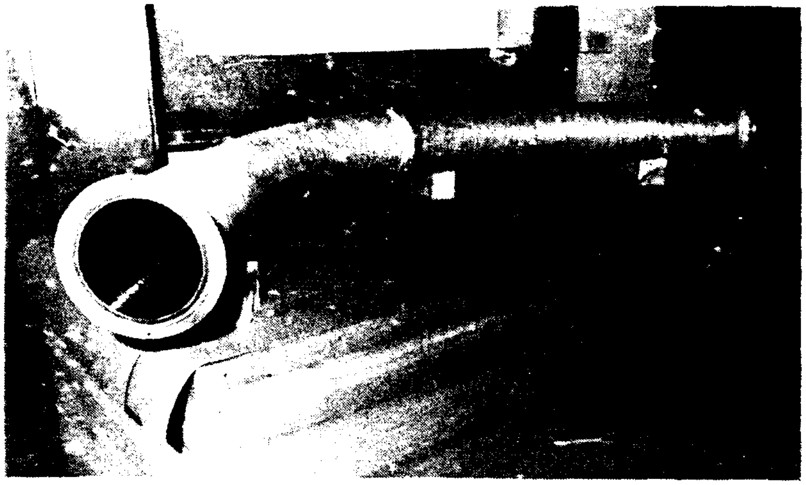

Figure 9 S-band sheathed-helix waveguide bend.

subtracted from that of the entire system to yield Δ.) Then a cavity is made by connecting endplates to the bend. The transmission coefficient of the cavity is of the form of Equation 1 with $M/8.68$ replacing $\alpha_{01}L$ and Δ replacing $\beta_{01}L$. Relations similar to Equations 3 and 4 may be derived from this cavity transmission coefficient. Determination of the bend insertion loss is expedited by comparing the Q of a bend cavity with that of a straight cavity. If one experimentally verifies that $d(\beta_{01}L)/d\omega = d\Delta/d\omega$ (as described above), then the following relation applies:

$$\left(\frac{Q_{\text{bend}}}{Q_{\text{straight}}}\right)^2 = \frac{\left(S_{22r}^2 + S_{22i}^2\right)^2 \exp(-2\alpha_{01}L) + \exp(2\alpha_{01}L) - 2\left(S_{22r}^2 - S_{22i}^2\right)}{\left(S_{22r}^2 + S_{22i}^2\right)^2 \exp(-M/8.68) + \exp(M/8.68) - 2\left(S_{22r}^2 - S_{22i}^2\right)} \tag{6}$$

Equation 6 was derived by neglecting $(\delta\omega)^2$ and finding the ratio of Equation 4 to the corresponding expression for a bend cavity. Making the approximations $S_{22r} = -1$, $S_{22i} = 0$, and using a series expansion of the exponential terms, Equation 6 reduces to the following:

$$M = 8.68\alpha_{01}L(Q_{\text{straight}} / Q_{\text{bend}}). \tag{7}$$

In Equation 7, M is in dB, and α_{01} is in Np/m. If the straight waveguide attenuation α_{01} is known, then Equation 7 may be used to determine the bend insertion loss M. In Section 2, Q measurements were used to establish lower and upper bounds on α_{01} for S-band sheathed-helix waveguide. The Q's of an S-band bend and a 7.32-ft S-band straight cavity have also been measured near 3.3 GHz (see Table 1). The extrapolated insertion loss value for the bend was in the range $0.027 \text{ dB} \leq M \leq 0.049$ dB. The theoretical loss (see Ref. 2, Eq. 1) is $M = 0.025$ dB. The actual bend loss may, in fact, be higher than this theoretical figure because the theory does not take into account the unavoidable exposure of the sheath caused by different portions of the wire separating from each other in the outer radius of a waveguide bend.

Table 1
Measured Q's for an S-band bend and a 7.32-ft S-band straight cavity. The movable conducting piston was adjusted so that both cavities were 7.32-ft long.

Frequency (MHz)	Q, Straight*	Q, Bend**
3283	24970	6950
3332	23070	6810

*Average Q = 24020. **Average Q = 6880.

4. FIXED–LENGTH STRAIGHT CAVITIES

In this section, the new model is used to extrapolate insertion loss values from the Q data of a fixed-length cavity. This approach differs from the previously described techniques principally in that S_{22_r} and S_{22_i} must be known before the measurements.

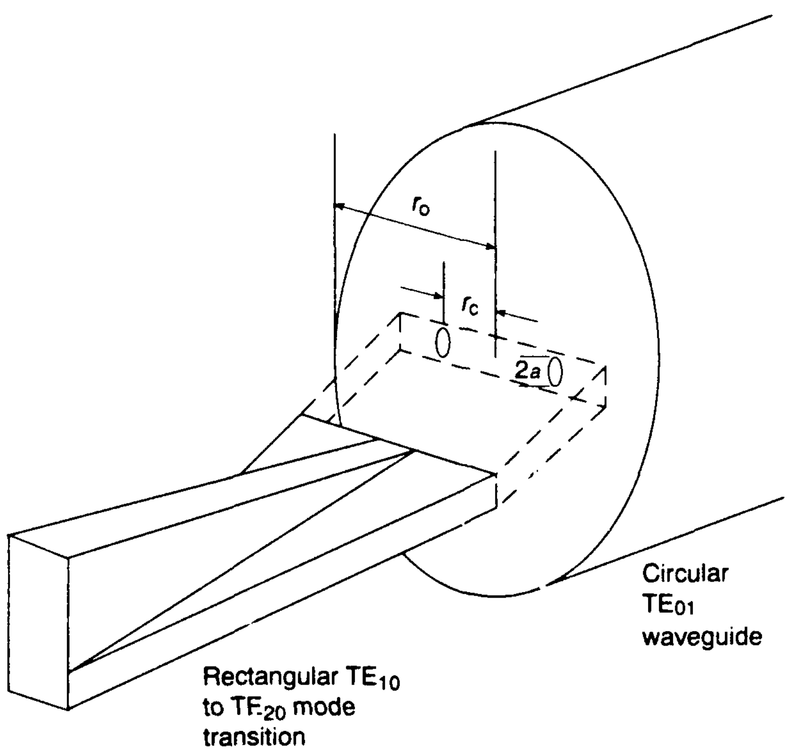

Figure 10 Endplate assembly used in fixed-length cavity tests. The aperture diameter $2a$ was equal to 0.635 cm, and r_c = 0.4804 r_o.

For these tests, the pair of coupling apertures shown in Figure 10 were used; the subscript "1" now refers to the rectangular TE_{20} mode. Using a quasistatic model, the following expression for S_{22} may be derived from Equation 61b on page 503 of Reference 9:

$$S_{22} = -1 + j\omega\gamma\mu_0 \mathbf{H}_n^+ \cdot \mathbf{M}\,. \tag{8}$$

Here, $\mathbf{M}$ is the magnetic dipole moment of the aperture (see Eqs. 69b and 72, pp. 507 and 508, of Ref. 9) and $\mathbf{H}_n^+$ is the magnetic field (suitably normalized) of the TE_{01} mode (Ref. 9, p. 359). The parameter γ is set equal to unity for conventional Bethe theory (e.g., Ref. 9); however, a model proposed by Collin (Ref. 9, pp. 508–511) may be used with the following result:

$$\gamma = \left(1 - j\frac{2}{9\pi}k_0^3 a^3\right)^{-1}, \tag{9}$$

where a is the aperture radius as shown in Figure 10. When Equation 9 is substituted into Equation 8, numerical verification that $|S_{22}|^2 < 1$ is possible. This condition is not met by the Bethe model. In any case, one may substitute these theoretical values for S_{22r} and S_{22i} into Equation 4; the additional substitution of a measured Q results in a quadratic equation in $\exp(-2\alpha_{01}L)$. A 4-ft-long, 12-cm-inner-diameter sheathed-helix waveguide cavity was observed to have a Q of 58477.0 at 4.42 GHz. Using Equation 9, the extrapolated value for α_{01} was 0.01085 dB/m as compared with a theoretical value of 0.0004762 dB/m. Improvement in the agreement between these two values could perhaps be achieved through the development of a better model for the aperture. The development of such an aperture model is being pursued.

5. CONCLUSIONS

A new model for interpreting data from a circular cylindrical cavity has been developed. This model is applicable to both fixed- and variable-length waveguide cavities. It is applicable to nonuniform cavities as long as the two endplates are of identical design. Experimental data have been presented, and the insertion loss values extrapolated from these data are in good agreement with the values predicted from the theory.

[9]R. E. Collin, *Field Theory of Guided Waves*, 2nd Ed., IEEE Press, New York (1991).

REFERENCES

[1]A. E. Karbowiak, and R. F. Skedd, "Testing of Circular Waveguides Using a Resonant Cavity Method," *Proc. IEE* **106B**, Supplement 13, 66–70 (Sep 1959).

[2]W. A. Huting, J. W. Warren, and J. A. Krill, "Recent Progress in Circular High-Power Overmoded Waveguide," *Johns Hopkins APL Tech. Dig.* **12**(1), 60–74 (1991).

[3]G. R. P. Marie, *Mode Transforming Waveguide Transition*, U. S. Patent No. 2,859,412, 4 Nov 1958.

[4]S. S. Saad, J. B. Davies, and O. J. Davies, "Analysis and Design of a Circular TE_{01} Mode Transducer," *IEE J. Microwaves Opt. Acoust.* **1**, 58–62 (Jan 1977).

[5]S. S. Saad, J. B. Davies, and O. J. Davies, "Computer Analysis of Gradually Tapered Waveguide with Arbitrary Cross Sections," *IEEE Trans. on Microwaves Theory Tech.* **MTT-25**, 437–440 (May 1977).

[6]R. H. Dicke, "General Microwave Theorems," in *Principles of Microwave Circuits*, C. G. Montgomery, R. H. Dicke, and E. M. Purcell (eds.), McGraw-Hill, New York, pp. 130–161 (1948).

[7]J. D. Jackson, *Classical Electrodynamics*, 2nd Ed., Wiley, New York (1975).

[8]*Model 360 Vector Network Analyzer Operation Manual*, Revision C, Wiltron Company, Morgan Hill, Ca., p. 1-9 (1987).

[9]R. E. Collin, *Field Theory of Guided Waves*, 2nd Ed., IEEE Press, New York (1991).

INITIAL DISTRIBUTION EXTERNAL TO THE APPLIED PHYSICS LABORATORY*

The work reported in TG 1383 was done under Navy Contract N00039-91-C-0001 and is related to Task BKHR9LXX-F2F, supported by The Johns Hopkins University Applied Physics Laboratory

ORGANIZATION	LOCATION	ATTENTION	No. of Copies
DEPARTMENT OF DEFENSE			
Defense Technical Information Center	Alexandria, VA 23314	Accessions	12
DEPARTMENT OF THE NAVY			
Naval Air Systems Command	Washington, DC 22202	Library, Air 7226	2
Naval Sea Systems Command O6C	NC-2 Crystal City, VA 20362	M. J. O'Driscoll	1
Naval Surface Warfare Center–Crane Division	Crane, IN 47522	G. Kreager	2
NAV TECH REP	Laurel, MD 20723-6099		2
SPAWAR	Arlington, VA 20363-5100	Library	2
OTHERS			
Purdue University	West Lafayette, IN 47907	K. J. Webb	1

Requests for copies of this report from DoD activities and contractors should be directed to DTIC. Cameron Station, Alexandria, Virginia 22314 using DTIC Form 1 and, if necessary, DTIC Form 55.

*Initial distribution of this document within the Applied Physics Laboratory has been made in accordance with a list on file in the APL Technical Publications Group.